RESEARCH ARTICLE

Effect of low temperature plasma on the transcriptome of breast cancer cells

Lei Liu[1, 2, †], Zhuna Yan[2, †], Yanhua Sun[1, †], Han Zhou[2], Hao Li[1, *], Wencheng Song[2, 3, *]

[1]School of Environment and Life Health, Anhui Vocational and Technical College, Hefei, Anhui, China. [2]Anhui Province Key Laboratory of Medical Physics and Technology, Center of Medical Physics and Technology, Hefei Institutes of Physical Science, Chinese Academy of Sciences, Hefei, Anhui, China. [3]Collaborative Innovation Center of Radiation Medicine of Jiangsu Higher Education Institutions and School for Radiological and Interdisciplinary Sciences, Soochow University, Suzhou, Jiangsu, China.

Received: December 26, 2024; **accepted:** April 26, 2025.

Breast cancer is one of the most diagnosed cancers in women. Due to the limitations of its therapeutic methods, new therapeutic method needs to be developed. More and more evidence has shown the potential of low-temperature plasma (LTP) in cancer treatment. This research investigated the inhibitory effect of LTP on the *in vitro* toxicity of breast cancer cells using the 3-(4,5-dimethylthiazol-2-yl)-2,5-diphenyltetrazolium bromide (MTT) assay, extracellular reactive oxygen species (ROS), and transcriptomics analysis. The results showed that, under 15 seconds, 30 seconds, and 45 seconds treatment, cell viability gradually decreased, while the extracellular ROS gradually increased. In addition, transcriptomic analysis results showed that 1,272 differentially expressed genes (DEGs), 1,573 DEGs, and 1,272 DEGs were obtained in the 15 s, 30 s, and 45 s treatment groups, respectively. The identified DEGs were involved in MAPK signaling pathway, Fox O signaling pathway, Wnt signaling pathway, TGF-beta signaling pathway, chemical carcinogenesis-reactive oxygen species and mTOR Signaling pathway. The results suggested that LTP inhibited cell viability and induced the differential gene expression in multiple signal transduction pathways, representing a potential new therapy for breast cancer.

Keywords: low-temperature plasma (LTP); transcriptomics analysis; enrichment; breast cancer; differential gene expression.

[*]**Corresponding author:** Hao Li, School of Environment and Life Health, Anhui Vocational and Technical College, Hefei 230011, Anhui, China. Wencheng Song, Anhui Province Key Laboratory of Medical Physics and Technology, Center of Medical Physics and Technology, Hefei Institutes of Physical Science, Chinese Academy of Sciences, Hefei 230031, Anhui, China. Email: lihao16@ustc.edu.cn (Li H), wencsong@cmpt.ac.cn (Song W).

[†]These authors contributed equally to this work.

Introduction

Breast cancer accounted for 11.7% of all malignancies globally in 2020, surpassing lung cancer to become the most diagnosed cancer worldwide [1]. In China, it ranks as the leading cancer among women, comprising 19.2% of all cases [2]. Breast cancer is classified using the TNM staging system (tumor size, lymph node involvement, distant metastasis) and molecular markers including estrogen receptor (ER), progesterone receptor (PR), and human epidermal growth factor receptor 2 (HER2) [3]. Current treatment modalities include breast-conserving surgery [4], chemoradiotherapy [5], and targeted therapies such as endocrine

therapy for ER-positive tumors and HER2-directed agents for HER2-overexpressing tumors [6]. However, systematic reviews have shown that breast-conserving therapy is associated with a higher risk of local recurrence compared to mastectomy [7]. Additionally, aggressive subtypes like triple-negative breast cancer (lacking ER, PR, and HER2 expression) are inherently metastatic and refractory to conventional therapies, underscoring the urgent need for innovative treatment strategies [8].

Low-temperature plasma (LTP), the fourth state of matter, exists beyond the solid, liquid, and gaseous phases. When subjected to an electric field exceeding the breakdown voltage, gas molecules ionize to generate a reactive mixture of electrons, ions, radicals, and excited atoms. This unique property has enabled the applications of LTP in diverse biomedical fields, notably in bactericidal treatment [9], wound healing [10], oncology [11], coagulation [12]. Emerging evidence underscores LTP's potential as a targeted cancer treatment with efficacy demonstrated in preclinical models of lung [13], melanoma [14], pancreatic [15], colorectal [16], esophageal cancers [17]. LTP exerts cytotoxic effects primarily through the generation of reactive oxygen and nitrogen species (RONS). Unlike normal cells, which maintain reactive oxygen species (ROS) levels below cytotoxic thresholds, cancer cells exhibit elevated baseline ROS due to oncogenic signaling and mitochondrial dysfunction. LTP further increases ROS/RONS production in cancer cells, surpassing their antioxidant capacity and triggering oxidative stress-mediated cell death [4]. This selective cytotoxicity toward cancer cells distinguishes LTP as a promising precision therapy. LTP has demonstrated selective cytotoxicity against metastatic (MDA-MB-231) and non-metastatic (MCF7) breast cancer cell lines by reducing cell viability, migration capacity, and perturbing vital cellular processes [18]. Phase I/II clinical trials further validate LTP's safety profile, showing no severe adverse reactions or systemic toxicity. Preclinical studies utilize the MTAG mouse model (MMTV-PyMT/B6), which recapitulates human breast cancer progression *via* MMTV-LTR promoter-driven polyomavirus T antigen expression [19]. This transgenic model is widely employed to investigate tumor-host immune interactions during breast cancer development [20]. LTP triggers multimodal cell death pathways in cancer cells.

Apoptosis is characterized by mitochondrial membrane depolarization, upregulated BAX/BCL2 ratios, and caspase-3 activation. G2/M cell cycle arrest further indicates impaired replicative capacity [21]. Oxidative stress plays a central role, as ROS generated by LTP exceeds the antioxidant capacity of cancer cells, leading to DNA damage (positive comet assay) and mitochondrial dysfunction [17, 22]. Signaling pathway modulation includes activation of Sestrin2/iNOS/Fas/p38 MAPK axes [23], while inhibition of prosurvival pathways (PI3K/AKT/mTOR, RAS/MEK) [24]. RNA-seq analysis of A875 melanoma cells revealed that LTP engaged multiple cell death programs including classical apoptosis *via* MAPK/p53 signaling [25], autophagic cell death marked by LC3B puncta formation, necroptosis characterized by RIPK1/RIPK3 phosphorylation. These findings were aligned with studies in B16F10 melanoma cells, where LTP-induced apoptosis involved caspase-3 activation through plasma-treated medium components [26]. Low-temperature plasma (LTP) represents a promising modality for breast cancer therapy, offering unique opportunities to advance low-dose oncologic mechanisms and facilitate translational interdisciplinary applications. However, key challenges including incomplete mechanistic understanding and limited preclinical validation hinder its clinical translation.

The AT-3 cell line derived from genetically engineered MTAG mice (MMTV-PyMT/B6) recapitulates human breast cancer progression with high fidelity including *in situ* tumorigenesis and spontaneous pulmonary metastasis. This murine model mirrors human breast cancer at

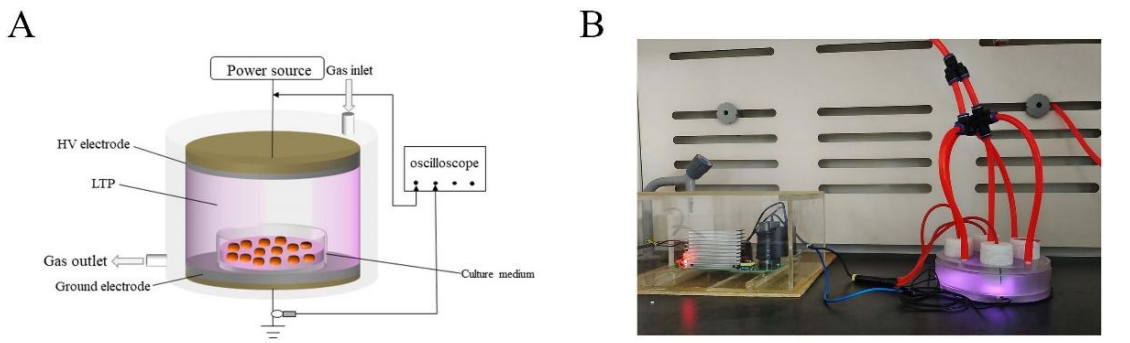

Figure 1. Schematic illustration of the low-temperature plasma (LTP) device (A) and photographic diagram of the LTP device in the laboratory setup (B).

the transcriptomic, proteomic, and tumor microenvironment levels, ensuring that LTP-induced transcriptomic signatures in AT-3 cells closely recapitulate human tumor responses. To address these gaps, this study systematically profiled LTP-responsive transcriptomic signatures in AT-3 cells. By integrating differential gene expression analysis with functional pathway enrichment, this research elucidated novel molecular mechanisms underlying LTP's anti-breast cancer effects, identified candidate biomarkers predictive of LTP treatment response, and provided preclinical validation for LTP-based precision oncology strategies. These findings would lay a critical foundation for advancing LTP from bench to bedside in breast cancer management.

Materials and methods

Cell culture

Mouse breast cancer AT-3 cells (Oricell, Shanghai, China) were maintained in Gibco Dulbecco's Modified Eagle Medium (DMEM) (Thermo Fisher Scientific, Waltham, MA, USA) supplemented with 10% fetal bovine serum (FBS) (Lonsera, Shanghai, China), 100 U/mL penicillin, and 100 μg/mL streptomycin. Cells were propagated in 60-mm culture dishes under standard conditions of 37°C, 5% CO_2, and 95% humidity in BB15 CO_2 incubator (Thermo Fisher Scientific, Waltham, MA, USA).

Low temperature plasma treatment

The low temperature plasma equipment designed for this research was schematically illustrated in Figure 1. Four plasma reactors were placed in a hollow quartz glass cylinder with two orifices in that reaction chamber including one for injecting experimental gases such as helium and one for exhausting gas from the reaction chamber. A ground electrode and a high-voltage electrode were included in the device, between which a low-temperature plasma with a high energy density was produced. The high-voltage electrodes were also covered with a 1 mm thick quartz glass as an insulating dielectric barrier. There were four holding grooves on the base with a 60 mm culture dish being placed in each groove. Helium with a purity of 99.999% was used with a gas flow rate of 1 L/min. Before the start of the experiment, Helium was introduced for 90 s to exhaust the air in the reaction chamber, and then the low-temperature plasma device was turned on. During the experiment, the medium was placed in a containment vessel of the low-temperature plasma device, and the cells were treated at predetermined intervals.

Cell viability experiments

Cell viability was evaluated using the 3-(4,5-dimethylthiazol-2-yl)-2,5-diphenyltetrazolium bromide (MTT) assay, which quantified mitochondrial dehydrogenase activity as a proxy for viable cell count. The MTT Cell Proliferation and Cytotoxicity Assay Kit (Sangon Biotech, Shanghai, China) was used according to the

manufacturer's protocol. Briefly, AT-3 cells were plated in 60-mm culture dishes and were grown to 70% confluence before being exposed to LTP for 15 s, 30 s, and 45 s. Treated cells were cultured under standard conditions for 24 hours. 1 mL of 0.5 mg/mL MTT solution was added to each dish and incubated at 37°C for 4 h to allow formazan crystal formation. After the aspiration of cultural media, 1 mL of DMSO was added to solubilize crystals. The absorbance at 490 nm was then measured using a Thermo Fisher Multiskan FC microplate reader (Thermo Fisher Scientific, Waltham, MA, USA).

Extracellular ROS detection

Extracellular H_2O_2 levels were determined using the Beyotime H_2O_2 Detection Kit (Beyotime Biotechnology, Shanghai, China) following the manufacturer's instructions. Briefly, AT-3 cells were grown to 70% confluence and treated with LTP for 0 s, 15 s, 30 s, and 45 s. The samples were collected by transferring 50 µL of conditioned medium to a 96-well plate immediately after treatment. 100 µL of pre-warmed H_2O_2 detection reagent at room temperature was added to each well. After incubating at 25°C, 50 rpm for 30 minutes in the dark, the absorbance at 560 nm was measured using a Thermo Fisher Multiskan FC microplate reader. H_2O_2 concentration was calculated from a standard curve generated with serial 0 - 100 µM dilutions of H_2O_2.

RNA extraction

After LTP treatments, cells were collected *via* centrifugation and stored at -80°C. Total RNA was extracted from these cells in triplicate using the TRIZOL kit (Invitrogen, Carlsbad, CA, USA) following the manufacturer's instructions. The quality of the extracted RNA was assessed using the Agilent 2100 bioanalytical system (Agilent, Santa Clara, CA, USA).

cDNA preparation and sequence

After treating total RNA with DNase I (Takara, Kusatsu, Shiga, Japan) to remove genomic DNA contamination, polyadenylated mRNA was then enriched using Oligo(dT) magnetic beads (Beyotime Biotech, Shanghai, China). mRNA libraries were constructed using the MGIEasy RNA Library Prep Kit (BGI, Shenzhen, Guangdong, China) following manufacturer's protocol. Briefly, mRNA was fragmented into 200 - 300 bp segments using fragmentation buffer. The first-strand cDNA was synthesized using random hexamer as the primer and reverse transcriptase. The second-strand cDNA was then synthesized using DNA polymerase I and RNase H to obtain double-stranded cDNA. After end repairing and A-tailing with 3'-adenine overhangs, the sequencing adapters with unique dual indexes were ligated to cDNA fragments. The libraries were amplified for 15 cycles using Phusion High-Fidelity DNA polymerase and then purified using AMPure XP beads (Beckman Coulter, Brea, CA, USA) and quantified using Qubit dsDNA HS Assay (Thermo Fisher Scientific, Waltham, MA, USA). Single-stranded circular DNA (sscDNA) was generated by rolling circle replication to form DNA nanoballs (DNBs) for sequencing on the DNBSEQ platform (MGI Tech, Shenzhen, Guangdong, China) in BGI (Shenzhen, Guangdong, China).

Transcriptome data analysis

Raw sequencing reads were first quality-controlled to ensure suitability for downstream analysis by removing the reads that were adapter sequences, with more than 5% unknown bases ("N"), and low-quality with Q ≤ 20 for more than 20% of bases. Clean reads were aligned to the Mus musculus reference genome (GRCm38.p6) using Hisat2 v2.2.1. Alignment metrics (https://daehwankimlab.github.io/hisat2/) for mapping rate and genome coverage and evaluated *via* SAMtools v1.16.1 (https://www.htslib.org/) to ensure data integrity. Gene expression levels were quantified using StringTie v2.2.1 (https://ccb.jhu.edu/software/stringtie/). The differential gene expressions were analyzed through pairwise comparisons between the control group and each of the three LTP treatment groups. Gene Ontology (GO) and Kyoto Encyclopedia of Genes and Genomes (KEGG) pathway enrichment were conducted using the BGI Multi-omics Platform

(https://www.bgi.com/) with GO analysis focusing on three domains including biological process (BP), cellular component (CC), molecular function (MF) and KEGG pathways identifying signaling networks perturbed by LTP treatment. Enrichment results were visualized by using ggplot2 v3.4.2 (https://ggplot2.tidyverse.org/) and clusterProfiler v4.6.2 (https://bioconductor.org/packages/release/bioc/html/clusterProfiler.html).

Statistical analysis

The gene expression profiles were compared using DESeq2 v1.38.3 (https://bioconductor.org/packages/release/bioc/html/DESeq2.html). The analysis employed a negative binomial generalized linear model to account for overdispersion in read counts followed by Benjamini-Hochberg correction for false discovery rate (FDR) to control type I error during multiple hypothesis testing. Genes with an adjusted *P* value (FDR) ≤ 0.05 and $|\log_2(\text{foldchange})| \geq 1$ were identified as differentially expressed genes (DEGs) in each treatment group relative to the control. Data was presented as mean ± SEM. Statistical significance was determined *via* one-way ANOVA followed by Tukey's post hoc test.

Results and discussion

Effect of LTP on cell viability

Cell viability was measured by MTT assay following 0 s, 15 s, 30 s, and 45 s of LTP exposure. The results showed that LTP induced a dose-responsive reduction in viability with 45 s treatment decreasing survival to 50.2 ± 3.1% of untreated controls (Figure 2). These results validated LTP's potential as a temporal precision therapy for breast cancer.

Impact of LTP on the generation of extracellular ROS

The extracellular H_2O_2 levels displayed a biphasic kinetic profile (Figure 3). In the first 0 – 15 s or rapid burst phase, H_2O_2 levels surged 12-fold to 36.0 ± 2.0 µM, while, in the 15 – 45 s or plateau phase, H_2O_2 concentration increased marginally to 45.0 ± 3.0 µM at 45 s. This kinetic pattern aligned with the cytotoxicity profile in Figure 2, where survival dropped to 50% at 45 s despite minimal H_2O_2 elevation beyond 30 s. These results highlighted ROS as a critical mediator of LTP-induced cell death.

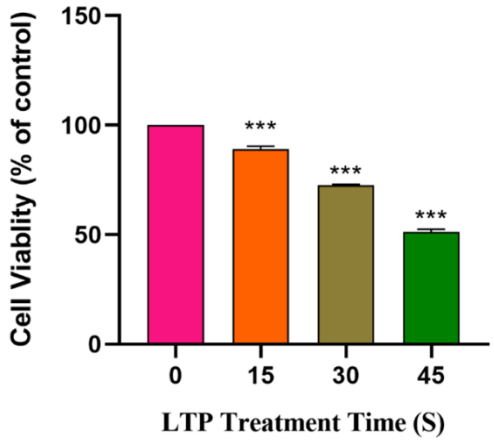

Figure 2. LTP elicited time-dependent cytotoxicity in breast cancer cells. $^{*}P < 0.05$, $^{**}P < 0.01$, $^{***}P < 0.001$ compared with the control.

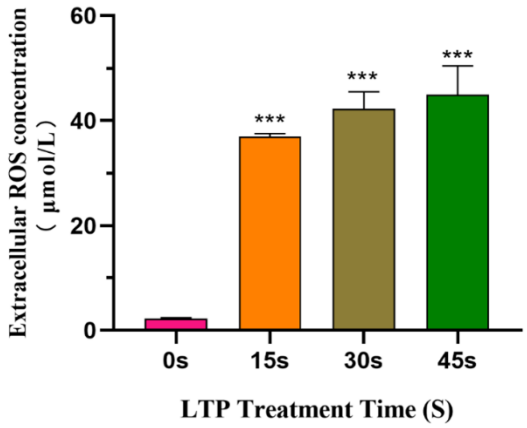

Figure 3. The concentrations of H_2O_2 in the cell culture media after LTP treatments. $^{*}P < 0.05$, $^{**}P < 0.01$, $^{***}P < 0.001$ compared with the control.

Transcriptome comparative analysis of breast cancer cells

Volcano plots were utilized to visualize differentially expressed molecules at 15 s, 30 s, and 45 s post-treatment versus the 0 s control

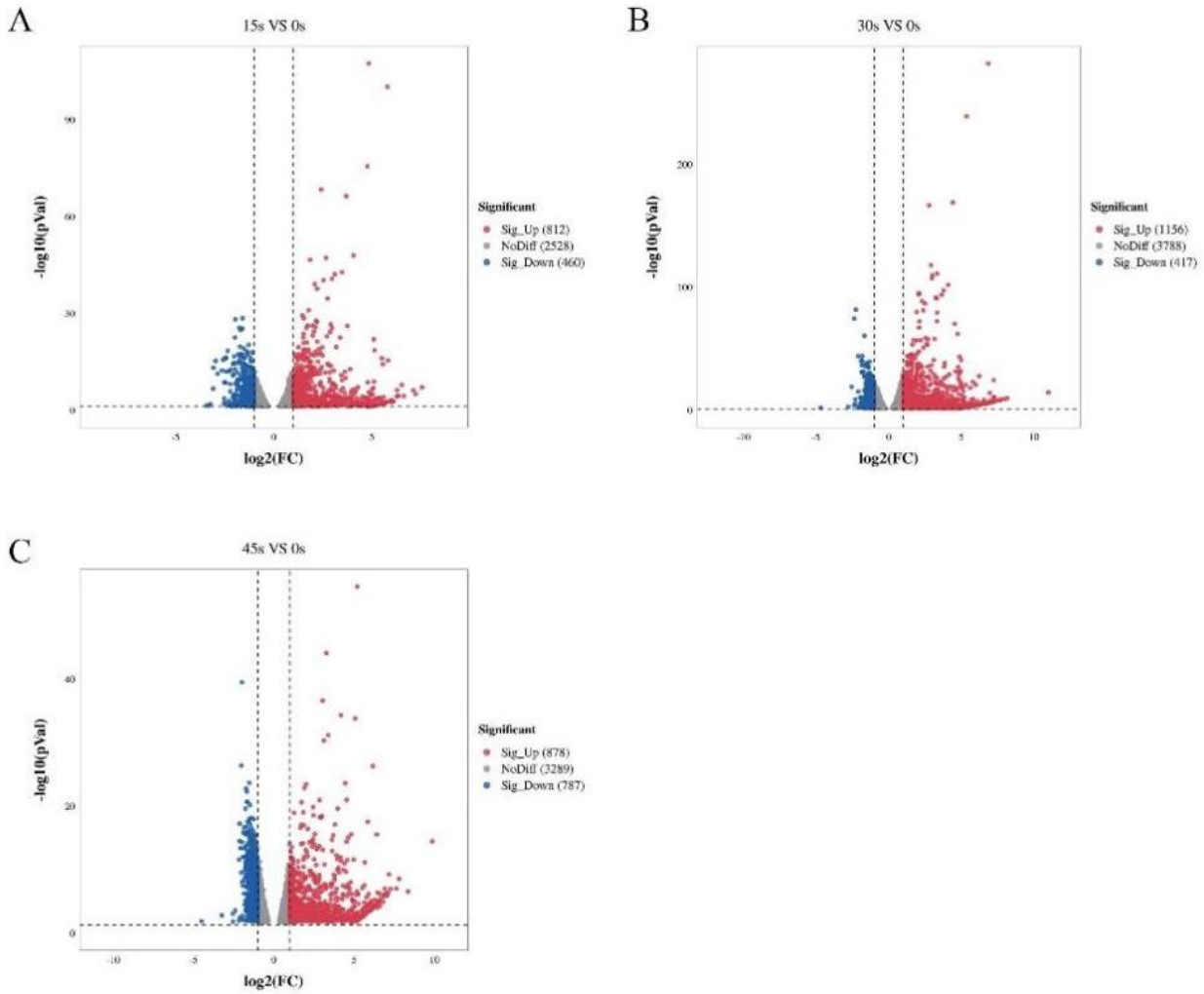

Figure 4. Volcano plots of differentially expressed genes in 15 s treatment (A), 30 s treatment (B), and 45 s treatment (C). Dashed lines marked the thresholds for statistical significance, $log_2FC = \pm 1$ (vertical) and $-log_{10}(P \text{ value}) = 1.3$ (horizontal).

group. In the group of 15 s after treatment (group A), a total of 812 molecules were significantly upregulated, while 460 molecules showed significant downregulation (Figure 4A). Most significantly altered molecules clustered in the moderate log_2FC range (0 – 5), indicating a dominant upregulation trend after 15 s treatment. In the group of 30 s treatment, the number of significantly upregulated molecules rose to 1,136 with only 117 molecules significantly downregulated (Figure 4B). Notably, some upregulated molecules exhibited higher log_2FC values (> 5), reflecting a more pronounced activation of molecular expression at the 30 s time point. In the group of 45 s treatment, there were 878 significantly upregulated molecules and 127 significantly downregulated ones (Figure 4C). The expanded log_2FC value distribution covered a broader range, indicating diverse expression responses to the 45 s treatment.

GO enrichment analysis of DEGs

GO enrichment analysis was conducted to elucidate the functional roles of DEGs under distinct treatment durations. In the 15 s treatment group, upregulated genes were significantly enriched in biological processes (BP) including the positive regulation of protein localization, cellular catabolic process, and protein-containing complex assembly.

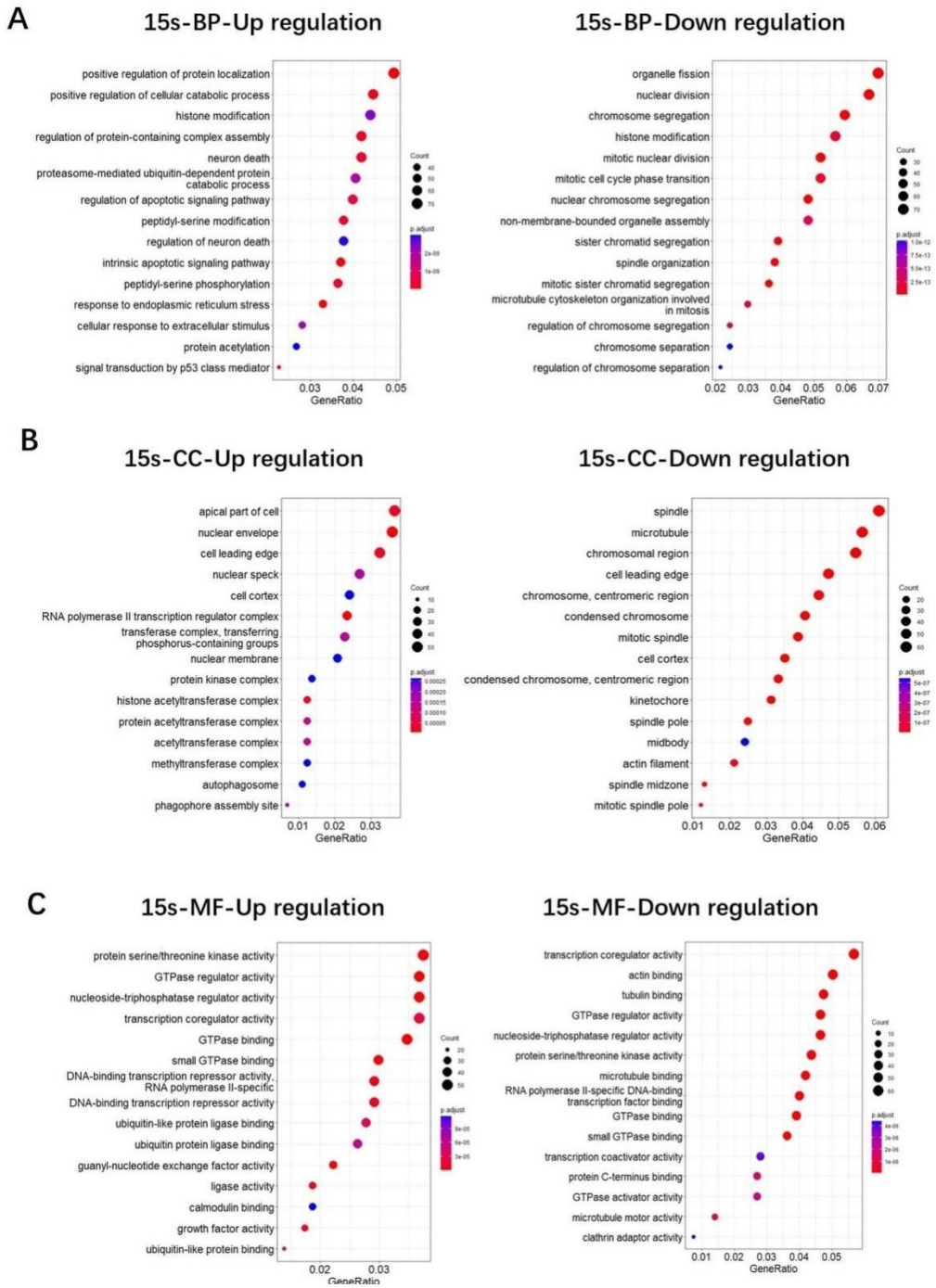

Figure 5. Gene Ontology (GO) enrichment analysis of AT-3 cells under 15 s treatment in biological process (BP) (A), cellular component (CC) (B), molecular function (MF) (C).

Downregulated genes were predominantly involved in organelle fission, nuclear division, and chromosome segregation (Figure 5A). Upregulated DEGs were associated with cellular components (CC) such as the apical part of the cell, nuclear envelope, and cell leading edge. In contrast, downregulated genes were linked to structures like the spindle, microtubule, and chromosomal region (Figure 5B). Both upregulated and downregulated genes

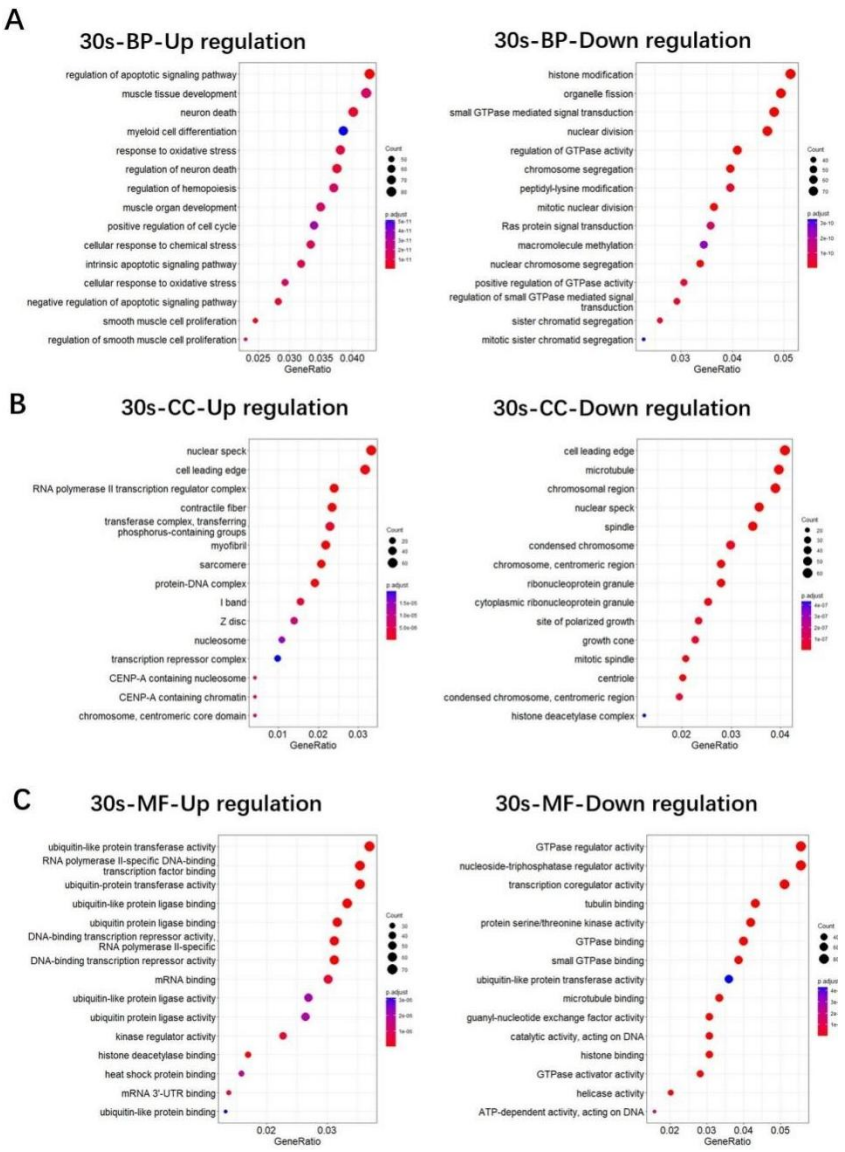

Figure 6. Gene Ontology (GO) enrichment analysis of AT-3 cells under 30 s treatment in biological process (BP) (A), cellular component (CC) (B), molecular function (MF) (C).

prominently participated in molecular functions including protein serine/threonine kinase activity, GTPase regulator activity, and transcription coregulator function (Figure 5C). In the 30 s treatment group, upregulated genes were involved in regulating the apoptotic signaling pathway, muscle tissue development, and neuron death, while downregulated genes were associated with histone modification, organelle fission, and small GTPase-mediated signal transduction in BP (Figure 6A). Upregulated genes were related to nuclear speck, cell leading edge, and RNA polymerase II transcription regulator complex, while downregulated genes were connected to the cell leading edge, microtubule, and chromosomal region in CC (Figure 6B). The upregulated genes primarily participated in ubiquitin-like protein ligase binding, DNA-binding transcription repressor activity, and mRNA binding, while downregulated genes were mainly involved in GTPase regulator activity, transcription coregulator activity, and tubulin binding in MF (Figure 6C). In the 45 s treatment group, the

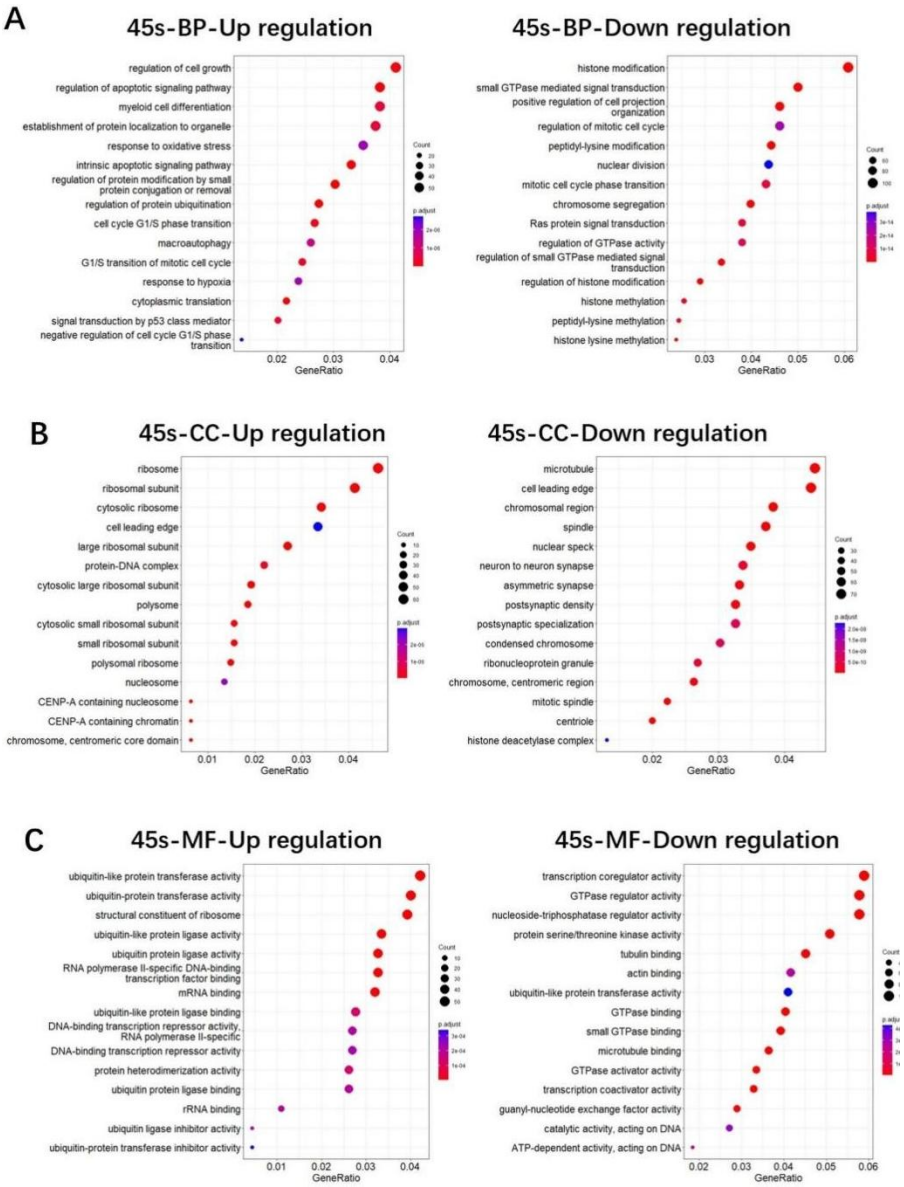

Figure 7. Gene Ontology (GO) enrichment analysis of AT-3 cells under 45s treatment in biological process (BP) (A), cellular component (CC) (B), molecular function (MF) (C).

upregulated genes were primarily associated with the regulation of cell growth, apoptotic signaling pathway, and myeloid cell differentiation. Downregulated genes were involved in histone modification, small GTPase-mediated signal transduction, and positive regulation of cell projection organization in BP (Figure 7A). The upregulated genes were linked to ribosome, protein-DNA complex, and ribosomal subunit in CC, while downregulated genes were associated with microtubule, cell leading edge, and chromosomal region (Figure 7B). The upregulated genes mainly participated in ubiquitin-like protein transfer activity, while downregulated genes were involved in transcription coregulator activity, GTPase regulator activity, and nucleoside-triphosphatase regulator activity in MF (Figure 7C). The GO enrichment analysis across the three experimental groups highlighted a critical trend

that genes related to the GTPase family were consistently downregulated. Existing research has shown that the GTPase family is significantly overexpressed in breast cancer tissues compared to healthy counterparts [27], and it plays pivotal roles in regulating cell migration and the cell cycle [28]. In this study, the downregulation of GTPase-related genes induced by LTP treatment suggested a potential anti-cancer mechanism. By reducing GTPase family expression, LTP might disrupt signaling pathways essential for breast cancer cell migration, thereby inhibiting metastatic potential. Additionally, the involvement of the GTPase family in cell cycle regulation implied that LTP might also interfere with cancer cell proliferation by altering cell cycle progression. These findings not only uncovered novel molecular targets of LTP in breast cancer treatment but also provided a theoretical basis for exploring LTP as a promising adjunct therapy. Further studies are warranted to validate the direct regulatory relationship between LTP and GTPase family members, as well as their downstream effects on cancer cell behavior.

KEGG pathway enrichment analysis of DEGs

KEGG pathway enrichment analysis was conducted to identify pivotal signaling pathways associated with DEGs with a *P* value less than 0.05 defined as the threshold for significant enrichment. In the 15 s treatment group, upregulated genes were prominently enriched in the MAPK signaling pathway, transcriptional misregulation in cancer, and FoxO signaling pathway (Figure 8A). Downregulated genes clustered in the cell cycle, Wnt signaling pathway, and Hippo signaling pathway (Figure 8B). In the 30 s treatment group, upregulated genes showed strong enrichment in transcriptional misregulation in cancer, the MAPK signaling pathway, and the FoxO signaling pathway (Figure 8C). Downregulated genes concentrated in the Rap 1 signaling pathway, TGF-β signaling pathway, and herpes simplex virus 1 infection pathway (Figure 8D). In the 45 s treatment group, upregulated genes were primarily enriched in pathways including ribosome, transcriptional misregulation in cancer, and chemical carcinogenesis–reactive oxygen species (Figure 8E). Downregulated genes were significantly associated with herpes simplex virus 1 infection and the mTOR signaling pathway (Figure 8F). The consistent enrichment of the MAPK signaling pathway in 15 s and 30 s groups' upregulated genes was critical, which governed cancer-related processes like proliferation, apoptosis, and inflammation with subfamilies such as p38, ERK, and JNK [29, 30]. The results aligned with Akter *et al*. who demonstrated that LTP inhibited U87 MG cell proliferation and upregulated MAPK-related apoptotic proteins [31]. The FoxO signaling pathway enriched in upregulated genes mediated apoptosis, cell cycle arrest, and antioxidant stress [32]. Its upregulation suppressed cell proliferation and invasion [33], and GWAS analyses suggested FoxO pathway components such as FBXO32 might be against breast cancer [34], indicating LTP's potential anti-cancer effects *via* FoxO activation. For downregulated genes, the Wnt signaling pathway enrichment in 15 s group was notable. The Wnt pathway drives breast cancer proliferation and metastasis [35], and its inhibition by LTP in this study suggested to reduce cancer cell migration. In the 30 s group, TGF-β pathway enrichment was significant. As a key cytokine in breast cancer [36], TGF-β inhibition by LTP might hinder cancer progression, which mirrored the resveratrol's effects on MDA231 cells [37]. In the 45 s group, the chemical carcinogenesis–ROS pathway enrichment in upregulated genes aligned with ROS's role in DNA damage and oxidative cell death [38]. Previous studies linked LTP's anti-myeloma effects to ROS induction [39], which consistent with ROS increase and cell viability decrease observed in this study. The mTOR pathway enrichment in 45 s group downregulated genes also matters, as mTOR alteration reduced cancer cell viability [40], reinforcing LTP's anti-cancer mechanism. Overall, LTP regulated multiple pathways including MAPK, FoxO, Wnt, TGF-β, ROS, and mTOR to inhibit breast cancer proliferation and migration. These findings laid a foundation for developing LTP as a novel breast cancer therapeutic strategy.

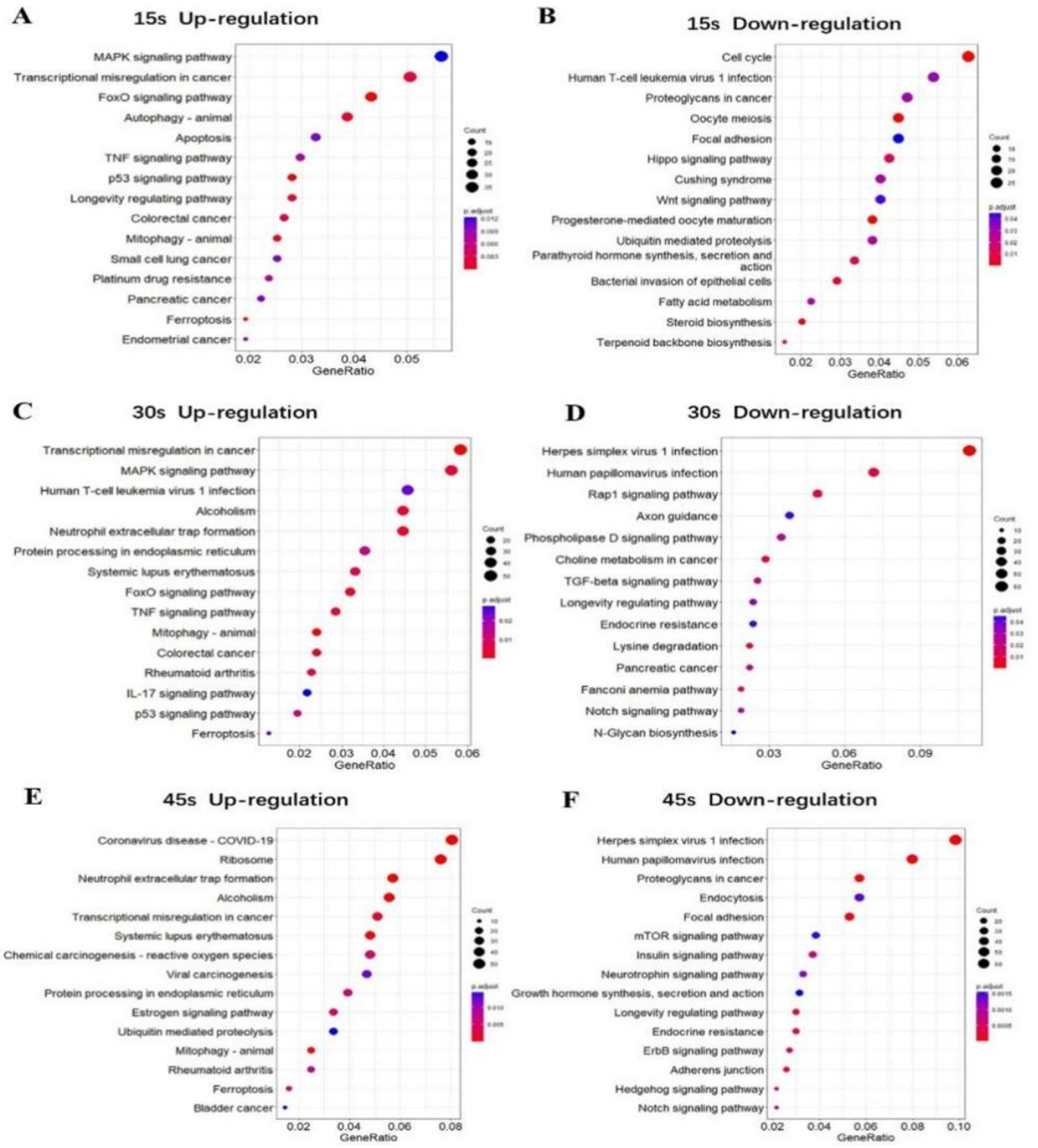

Figure 8. KEGG pathway enrichment analysis for upregulated genes in the 15 s treatment group (A), downregulated genes in the 15s treatment group (B), upregulated genes in the 30 s treatment group (C), downregulated genes in the 30 s treatment group (D), upregulated genes in the 45 s treatment group (E), downregulated genes in the 45 s treatment group (F).

Conclusion

This study systematically investigated the effects of low-temperature plasma (LTP) on breast cancer cells, integrating cellular, molecular, and omics analyses to unravel LTP anti-cancer mechanisms. The results demonstrated a time-dependent reduction in cell viability driven by a biphasic increase in extracellular ROS, which established ROS as a critical mediator of LTP-

induced cytotoxicity. Transcriptomic profiling demonstrated dynamic gene expression changes in different LTP treatments and differentially expressed genes (DEGs), respectively, with pronounced enrichment in pathways linked to cancer progression. GO enrichment analysis highlighted a consistent downregulation of GTPase-related genes across all treatment groups, which overexpressed in breast cancer and implicated in cell migration and cell cycle regulation. This result suggested that LTP might inhibit metastatic potential and proliferation by dampening GTPase-dependent signaling. KEGG pathway analysis further identified multiple targets including upregulated MAPK and FoxO pathways that promoted apoptosis and cell cycle arrest, while downregulated Wnt, TGF-β, and mTOR pathways that disrupted oncogenic processes like migration and survival. Collectively, these results demonstrated that LTP exerted anti-cancer effects through a multi-mechanistic approach, integrating ROS-mediated cytotoxicity with transcriptional reprogramming of key signaling networks. The study provided a robust foundation for developing LTP as a temporal precision therapy for breast cancer with future research warranted to validate direct interactions between LTP and GTPase family members, as well as downstream functional impacts on cancer cell behavior.

Acknowledgements

This study was supported by the Natural Science Foundation of China (Grant No. 22142007 and 22006001), the Anhui Province University Natural Science Research Project (Grant No. 2022AH040277, 2022AH052058, and 2023AH040193), and the Collaborative Innovation Center of Radiation Medicine of Jiangsu Higher Education Institutions.

References

1. Sung H, Ferlay J, Siegel RL, Laversanne M, Soerjomataram I, Jemal A. 2021. Global Cancer Statistics 2020: GLOBOCAN Estimates of Incidence and Mortality Worldwide for 36 Cancers in 185 Countries. CA Cancer J Clin. 71(3):209-249.
2. Qiu HB, Cao SM, Xu RH. 2021. Cancer incidence, mortality, and burden in China: A time-trend analysis and comparison with the United States and United Kingdom based on the global epidemiological data released in 2020. Cancer Commun. 41(10):1037-1048.
3. Tsang JYS, Tse GM. 2020. Molecular classification of breast cancer. Adv Anat Pathol. 27(1):27-35.
4. Kim HW, Jeong D, Ham J, Kim H, Ji HW, Choi EH. 2020. ZNRD1 and its antisense long noncoding RNA ZNRD1-AS1 are oppositely regulated by cold atmospheric plasma in breast cancer cells. Oxid Med Cell Longev. 2020:9490567.
5. Jornet D, Loap P, Pierga JY, Laki F, Vincent-Salomon A, Kirova YM. 2021. Neoadjuvant concurrent radiotherapy and chemotherapy in early breast cancer patients: Long-term results of a prospective phase II trial. Cancers (Basel). 13(20):5107.
6. Wockel A, Albert US, Janni W, Scharl A, Kreienberg R, Stuber T. 2018. The screening, diagnosis, treatment, and follow-up of breast cancer. Dtsch Arztebl Int. 115(18):316-323.
7. Wang C, Lin Y, Zhu H, Zhou Y, Mao F, Huang X, *et al*. 2022. Breast-conserving therapy for breast cancer with BRCA mutations: A meta-analysis. Breast Cancer. 29(2):314-323.
8. Waks AG, Winer EP. 2019. Breast cancer treatment: A review. JAMA. 321(3):288-300.
9. Nicol MJ, Brubaker TR, Honish BJ, 2nd, Simmons AN, Kazemi A, Geissel MA, *et al*. 2020. Antibacterial effects of low-temperature plasma generated by atmospheric-pressure plasma jet are mediated by reactive oxygen species. Sci Rep. 10(1):3066.
10. Liu JR, Xu GM, Shi XM, Zhang GJ. 2017. Low temperature plasma promoting fibroblast proliferation by activating the NF-kappaB pathway and increasing cyclinD1 expression. Sci Rep. 7(1):11698.
11. Nam SH, Ok SM, Kim GC. 2018. Tooth bleaching with low-temperature plasma lowers surface roughness and Streptococcus mutans adhesion. Int Endod J. 51(4):479-488.
12. Moloney JN, Cotter TG. 2018. ROS signaling in the biology of cancer. Semin Cell Dev Biol. 80:50-64.
13. Yang Y, Li D, Li Y, Jiang Q, Sun R, Liu J, *et al*. 2020. Low-temperature plasma suppresses proliferation and induces apoptosis in lung cancer cells by regulating the miR-203a/BIRC5 axis. Onco Targets Ther. 13:5145-5153.
14. Yan D, Wang Q, Adhikari M, Malyavko A, Lin L, Zolotukhin DB, *et al*. 2020. A physically triggered cell death *via* transbarrier cold atmospheric plasma cancer treatment. ACS Appl Mater Interfaces. 12(31):34548-34563.
15. Liedtke KR, Bekeschus S, Kaeding A, Hackbarth C, Kuehn JP, Heidecke CD, *et al*. 2017. Non-thermal plasma-treated solution demonstrates antitumor activity against pancreatic cancer cells *in vitro* and *in vivo*. Sci Rep. 7(1):8319.
16. Wang Y, Mang X, Li X, Cai Z, Tan F. 2022. Cold atmospheric plasma induces apoptosis in human colon and lung cancer cells through modulating mitochondrial pathway. Front Cell Dev Biol. 10:915785.

17. Estarabadi H, Atyabi SA, Tavakkoli S, Noormohammadi Z, Gholami MR, Ghiaseddin A. 2021. Cold atmospheric plasma induced genotoxicity and cytotoxicity in esophageal cancer cells. Mol Biol Rep. 48(2):1323-1333.
18. Terefinko D, Dzimitrowicz A, Bielawska-Pohl A, Klimczak A, Pohl P, Jamroz P. 2021. The influence of cold atmospheric pressure plasma-treated media on the cell viability, motility, and induction of apoptosis in human non-metastatic (MCF7) and metastatic (MDA-MB-231) breast cancer cell lines. Int J Mol Sci. 22(8):3855.
19. Guy CT, Cardiff RD, Muller WJ. 1992. Induction of mammary tumors by expression of polyomavirus middle T oncogene: A transgenic mouse model for metastatic disease. Mol Cell Biol. 12(3):954-961.
20. Stewart TJ, Abrams SI. 2007. Altered immune function during long-term host-tumor interactions can be modulated to retard autochthonous neoplastic growth. J Immunol. 179(5):2851-2859.
21. Almeida-Ferreira C, Silva-Teixeira R, Goncalves AC, Marto CM, Sarmento-Ribeiro AB, Caramelo F, *et al*. 2022. Cold atmospheric plasma apoptotic and oxidative effects on MCF7 and HCC1806 human breast cancer cells. Int J Mol Sci. 23(3):1698.
22. Zhen X, Sun HN, Liu R, Choi HS, Lee DS. 2020. Non-thermal plasma-activated medium induces apoptosis of Aspc1 cells through the ROS-dependent autophagy pathway. *In Vivo*. 34(1):143-153.
23. Xia J, Zeng W, Xia Y, Wang B, Xu D, Liu D, *et al*. 2019. Cold atmospheric plasma induces apoptosis of melanoma cells *via* Sestrin2-mediated nitric oxide synthase signaling. J Biophotonics. 12(1):e201800046.
24. Adhikari M, Adhikari B, Ghimire B, Baboota S, Choi EH. 2020. Cold atmospheric plasma and silymarin nanoemulsion activate autophagy in human melanoma cells. Int J Mol Sci. 21(6):1939.
25. Zhao L, Yan C, Kong S, Jia T, Chu Z, Yang L, *et al*. 2022. Biosafety and differentially expressed genes analysis of melanoma cells treated with cold atmospheric plasma. J Biophotonics. 15(6):e202100403.
26. Mahdikia H, Shokri B, Majidzadeh AK. 2021. The feasibility study of plasma-activated water as a physical therapy to induce apoptosis in melanoma cancer cells *in-vitro*. Iran J Pharm Res. 20(3):337-350.
27. Ebrahimi N, Kharazmi K, Ghanaatian M, Miraghel SA, Amiri Y, Seyedebrahimi SS, *et al*. 2022. Role of the Wnt and GTPase pathways in breast cancer tumorigenesis and treatment. Cytokine Growth Factor Rev. 67:11-24.
28. Kazmi N, Robinson T, Zheng J, Kar S, Martin RM, Ridley AJ. 2022. Rho GTPase gene expression and breast cancer risk: A Mendelian randomization analysis. Sci Rep. 12(1):1463.
29. Peluso I, Yarla NS, Ambra R, Pastore G, Perry G. 2019. MAPK signaling pathway in cancers: Olive products as cancer preventive and therapeutic agents. Semin Cancer Biol. 56:185-195.
30. Ke J, Han W, Meng F, Guo F, Wang Y, Wang L. 2021. CTI-2 inhibits metastasis and epithelial-mesenchymal transition of breast cancer cells by modulating MAPK signaling pathway. Int J Mol Sci. 22(22):12229.
31. Akter M, Jangra A, Choi SA, Choi EH, Han I. 2020. Non-thermal atmospheric pressure bio-compatible plasma stimulates apoptosis *via* p38/MAPK mechanism in U87 malignant glioblastoma. Cancers (Basel). 12(1):245.
32. Guo W, Yao X, Lan S, Zhang C, Li H, Chen Z, *et al*. 2022. Metabolomics and integrated network pharmacology analysis reveal SNKAF decoction suppresses cell proliferation and induced cell apoptosis in hepatocellular carcinoma *via* PI3K/Akt/P53/FoxO signaling axis. Chin Med. 17(1):76.
33. Shan Z, Li Y, Yu S, Wu J, Zhang C, Ma Y, *et al*. 2019. CTCF regulates the FoxO signaling pathway to affect the progression of prostate cancer. J Cell Mol Med. 23(5):3130-3139.
34. Wang H, Liu H, Zhao L, Luo S, Akinyemiju T, Hwang S, *et al*. 2021. Association of genetic variants of FBXO32 and FOXO6 in the FOXO pathway with breast cancer risk. Mol Carcinog. 60(10):661-670.
35. Xu X, Zhang M, Xu F, Jiang S. 2020. Wnt signaling in breast cancer: biological mechanisms, challenges and opportunities. Mol Cancer. 19(1):165.
36. Shukla N, Naik A, Moryani K, Soni M, Shah J, Dave H. 2022. TGF-beta at the crossroads of multiple prognosis in breast cancer, and beyond. Life Sci. 310:121011.
37. Sun Y, Zhou QM, Lu YY, Zhang H, Chen QL, Zhao M. 2019. Resveratrol inhibits the migration and metastasis of MDA-MB-231 human breast cancer by reversing TGF-beta1-induced epithelial-mesenchymal transition. Molecules. 24(6):1131.
38. Srinivas US, Tan BWQ, Vellayappan BA, Jeyasekharan AD. 2019. ROS and the DNA damage response in cancer. Redox Biol. 25:101084.
39. Qi M, Zhao X, Fan R, Zhang X, Peng S, Xu D. 2022. Cold atmospheric plasma suppressed MM *in vivo* engraftment by increasing ROS and inhibiting the Notch signaling pathway. Molecules. 27(18):5832.
40. Yoshikawa N, Liu W, Nakamura K, Yoshida K, Ikeda Y, Tanaka H, *et al*. 2020. Plasma-activated medium promotes autophagic cell death along with alteration of the mTOR pathway. Sci Rep. 10(1):1614.